Electrical Power and Energy Systems 118 (2020) 105763

Contents lists available at ScienceDirect

Electrical Power and Energy Systems

journal homepage: www.elsevier.com/locate/ijepes

Multi-timescale coordinated schedule of interdependent electricity-natural gas systems considering electricity grid steady-state and gas network dynamics☆

Zhejing Bao[a], Yangli Ye[a], Lei Wu[b,*]

[a] College of Electrical Engineering, Zhejiang University, Hangzhou 310027, China
[b] Electrical and Computer Engineering Department, Stevens Institute of Technology, NJ07030, USA

ARTICLE INFO

Keywords:
Coordinated scheduling
Gas dynamics
Integrated electricity-natural gas system
Uncertainty
Wind power

ABSTRACT

The tight interdependency between electricity and natural gas systems brings new operation challenges to coordinate the two systems for achieving optimized multi-energy supply. The coordinated short-term schedule and real-time dispatch of an integrated electricity-natural gas system (IEGS) with energy coupling components (i.e., P2G (power to gas) assets and gas-fired generators) are proposed. Specifically, in the short-term schedule, electricity generators and gas sources are optimized in a unified model to achieve the minimal operation cost, where prevailing operation constraints related to hourly-scale steady-state power flow and minute-scale gas transmission dynamics are satisfied and extreme wind power scenarios are also considered. In the real-time dispatch, P2G assets and gas-fired generators are optimized to smooth the wind power forecast errors, aiming at mitigating impacts of wind power uncertainties on gas pressures variations. Through real-time dispatch, extreme wind power scenarios which cause violations of gas pressures will be identified and fed back to the short-term schedule problem, seeking for new operation strategies that would mitigate potential gas pressure violations induced by wind power uncertainties in real time. An IEGS, consisting of a 15-node and 14-pipeline natural gas network and a 24-bus and 35-branch power network, is established to validate the proposed approach. Simulation results demonstrate that linepack, P2G, and gas-fired generators can be utilized to effectively enhance operational economics and robustness of IEGS against uncertainties.

1. Introduction

Among various primary energy sources, natural gas has received more attentions owing to its abundant reserves, convenience to store, high energy conversion efficiency, and low pollutant emission. To this end, the share of natural gas in electric power generation has gradually increased, which has significantly intensified the coupling between natural gas and electric power systems [1]. Indeed, researches have shown that electricity and natural gas coupled system can entail lower investment costs as compared to traditional independent systems [2]. Consequently, coordinated optimal scheduling of natural gas, electricity, and other energy resources is of great interests for improving energy utilization efficiency and ensuring energy supply reliability.

The integrated electricity-natural gas system (IEGS) has attracted wide attentions in industry and academia. In IEGS, gas-fired power plants, P2G (power to gas) technology, and linepack of natural gas pipelines can provide a great deal of flexibility to enhance economic and reliable operations [3,4]. Indeed, gas-fired generators and P2G assets can realize the large-scale interconversion of electricity energy and natural gas, and the inherit storage capacity of the natural gas network can help mitigate fluctuations of renewable energy as well as gas and electricity demands, thus forming a cost-efficient and reliable integrated energy system [5–7].

Recently, many scholars have implemented relevant research on energy flow analysis as well as optimal planning and operation of IEGS. A Newton-Raphson based approach was described in [8,9] to analyze the steady-state energy flow of IEGS. An expansion planning approach for IEGS was proposed in [10] to minimize infrastructure expansion and operation costs over the entire time horizon. A planning model for IEGS, formulated as a two-stage robust optimization problem, was proposed in [11] to enhance power grid resilience under extreme conditions. Two interval-based uncertainty analysis methods were

☆ This work was supported by the National Natural Science Foundation of China under Grant No. 51777182, and in part supported by the U.S. National Science Foundation under Grant No. CMMI-1906780.

* Corresponding author.
E-mail address: lei.wu@stevens.edu (L. Wu).

https://doi.org/10.1016/j.ijepes.2019.105763
Received 18 July 2019; Received in revised form 9 October 2019; Accepted 7 December 2019
Available online 17 December 2019
0142-0615/

presented in [12] to study the impact of wind power on steady-state operation of IEGS. A unit commitment and economic dispatch framework coupled with an energy flow model of natural gas network was developed in [13]. A security-constrained economic dispatch model for IEGS was proposed in [14], formulated as a bi-level optimization problem with day-ahead electricity economic dispatch at the upper level and optimal allocation of natural gas at the lower level. A security-constrained unit commitment model combined with natural gas network constraints was proposed in [15]. A security-constrained unit commitment formulation was proposed in [16], which was solved by Bender's decomposition through a master problem to handle power constraints and subproblems to check gas network constraints. An optimization model was developed in [17] to capture spatiotemporal interactions between gas and electricity transmission networks, in which electricity and gas dispatch were solved separately.

When analyzing the coordinate operation of IEGS, it is important to recognize that response times of electric power and natural gas systems are significantly different. Indeed, as electrical system time constant is relatively small, following a disturbance the power grid can reach a new steady state almost instantaneously; on the contrary, natural gas flow is a much slower process, with the propagation of pressure and gas flow changes around 350 m/s [18], resulting in a much longer transient time in response to fluctuations. Thus, in recognizing the effects of natural gas dynamics on generation scheduling in IEGS, the characteristics of power flow and gas transmission at different timescales need to be considered simultaneously. Gas network dynamics was analyzed in [19] by transforming spatial partial differential equations into finite difference equations. A dynamic optimal energy flow model for IEGS was proposed in [20] by combining transient gas flow and steady-state power flow, which was transformed into a single stage linear programming problem with a unified timescale. A combined quasi-dynamic simulation model was introduced in [18], including a transient hydraulic model for gas system and an AC-optimal power flow based steady-state electric power model. An optimal electricity-gas coordinated scheduling was introduced in [21] considering electricity transmission N-1 contingencies and gas dynamics, which was solved by a two-stage linearized method. Considering wind power uncertainties and dynamic security constraints of the gas network, a two-stage robust generation scheduling was proposed in [22] to explore the effect of gas flow dynamics in robust generation scheduling.

Reviewing the above existing research, the work on coordinated operation of P2G, gas-fired generators, and linepack to achieve economic operation of IEGS while effectively mitigating wind energy uncertainties is rather limited. Specially, since linepack can only be accurately quantified by the description of gas transmission dynamics at a short timescale, a unified co-optimization model, integrating electricity transmission and gas delivering at different timescales, is in urgent need.

This paper focuses on a multi-timescale optimization framework of IEGS, in which short-term schedule and real-time dispatch are coordinated to achieve operational economics and robustness against wind power uncertainties. In short-term schedule of IEGS, a unified optimization model is developed in which the hourly-scale steady-state electricity transmission and minute-scale dynamical gas delivery are integrated to achieve economic operation, while considering the forecasted and extreme scenarios of wind power. Specifically, the minute-scale mass flow rates at P2G and gas-fired generator nodes are coupled with their corresponding hourly-scale electric power consumption and generation. In real-time dispatch, operation of P2G assets and gas-fired generators are optimized to smooth out wind power forecasting errors, i.e., their outputs are adaptively adjusted to ensure that gas pressures deviate from their short-term scheduled values as small as possible. In both short-term schedule and real-time dispatch, owing to gas compressibility, linepack will offer flexibility to enhance economic operation and mitigate wind energy uncertainty. The coordination between short-term schedule and real-time dispatch is realized by the closed-loop iterative framework, i.e. real-time dispatch takes short-term schedule results as input, while extreme wind power scenarios identified from real-time dispatch are fed back to short-term schedule to design new economic scheduling results that are robust against extreme wind power scenarios. The iterative procedure terminates when no new extreme scenario is identified in the real-time dispatch problem.

The remainder of this paper is organized as follows. Section 2 illustrates multi-timescale coordinated scheduling of IEGS from two aspects. Section 3 describes the optimization models of short-term scheduling and real-time dispatch for IEGS, while considering prevailing unit commitment constraints, steady-state DC power flow constraints, and transient gas transmission constraints. Simulation results are presented in Section 4. Section 5 draws the conclusions.

2. Multi-timescale coordinated schedule of IEGS

Multi-timescale coordination of IEGS scheduling can be illustrated via the following two aspects.

(i) The short-term schedule and the real-time dispatch are coordinated by identifying extreme scenarios of wind power from real-time dispatch and adding into short-term scheduling optimization iteratively, until no new extreme scenarios arise, as shown in Fig. 1. Specifically, the objective of the short-term schedule is to achieve economic operation while considering forecasted values and the extreme scenarios of wind power as well as operation constraints of steady-state electricity transmission network and gas delivering dynamics. In real-time dispatch, P2G assets and gas-fired generators are utilized to smooth the minute-scale fluctuations of wind power, aiming to minimize the deviation of pressure in gas network from the scheduled one. In summary, wind power uncertain is mitigated via two ways, i.e. considering hourly-scale extreme scenarios in short-term schedule and smoothing minute-scale fluctuation by utilizing P2G, gas-fired generators, and linepack in real-time dispatch.

(ii) In the short-term schedule, the steady-state power flow and the transient gas flow of different timescales are combined in a single optimization model. With hourly forecasts on wind power generation as well as natural gas and electricity demands, the integrated coordination schedule is implemented to determine hourly optimal electricity generation, P2G operation, and gas source mass flow rates, which minimize the total operation costs while satisfying constraints of steady-state electricity power flow and natural gas transmission dynamics. The reasons for combining the steady-state power flow and transient gas flow at different timescales into a single optimization model can be understood from two aspects: (a) When electricity demands or generations change, the transition process in the electricity system can be completed in milliseconds; however, the resulted operational changes of the corresponding

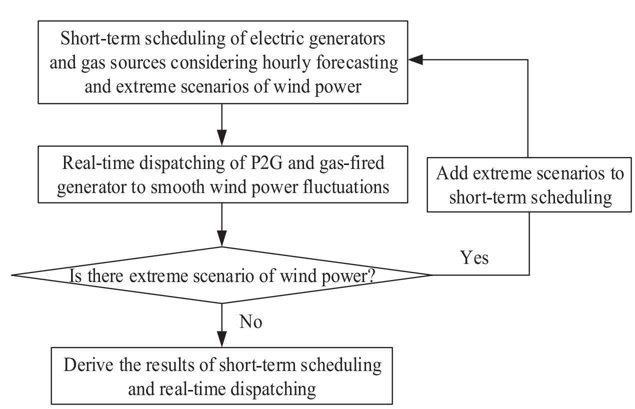

Fig. 1. Coordinated short-term schedule and real-time dispatch of an IEGS.

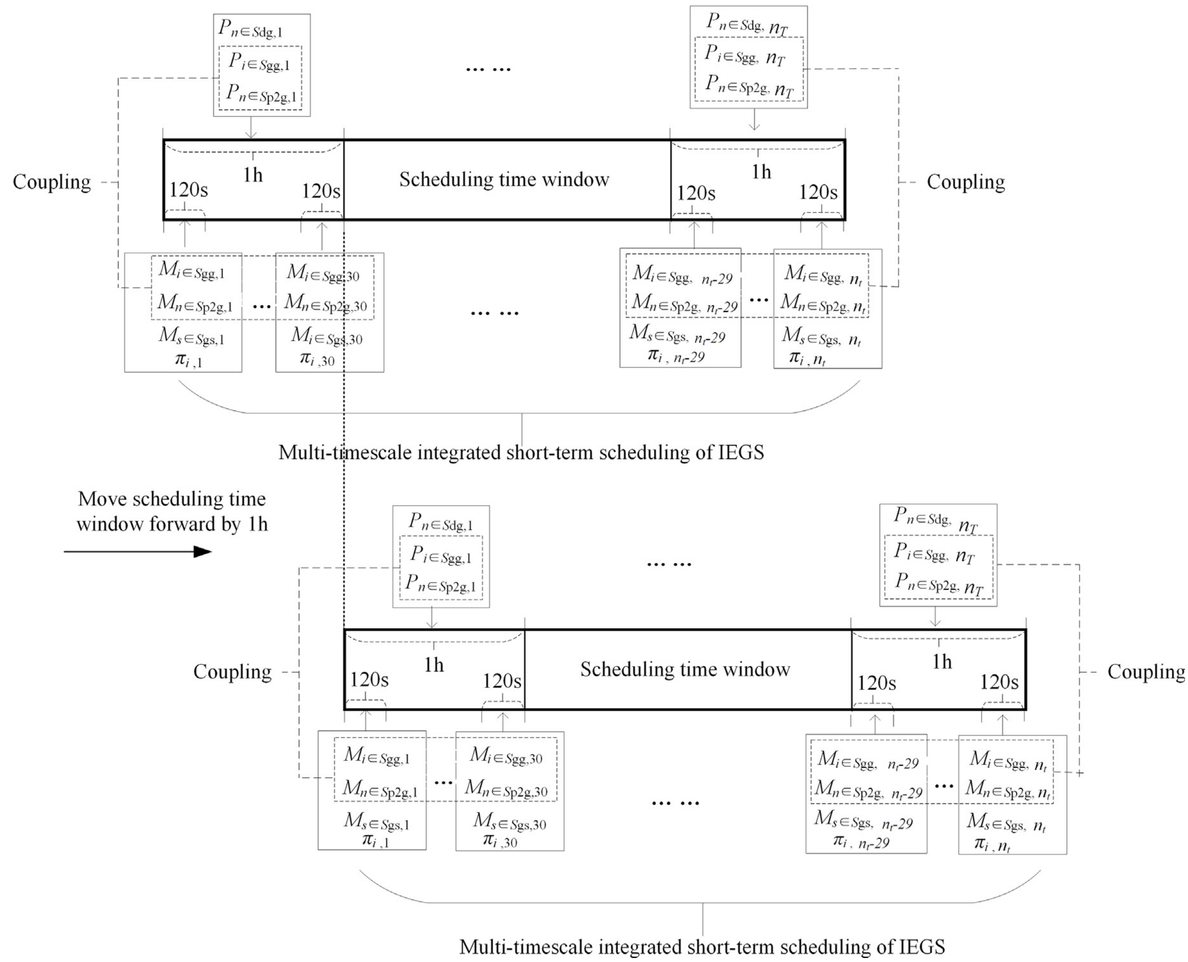

Fig. 2. Multi-timescale coordinated short-term scheduling of IEGS.

energy coupling components in the gas network would lead to a slower dynamical transmission process; (b) Because linepack of gas pipelines is enabled by gas compressibility, in order to accurately quantify linepack of gas pipelines and analyze its contribution to the optimal operation of IEGS, the dynamic mass flow rates and gas pressures in the gas network need to be adequately considered.

The multi-timescale coordination of the IEGS short-term scheduling is described in Fig. 2. Specifically, in the short-term scheduling time window spanning n_T hours, time resolution of the electricity variables, including power outputs of generators and electric consumptions of P2G, is one hour, while time resolution Δt of natural gas variables, such as mass flow rates and gas pressures, is in minute-scale. The gas dynamics model, which will be discussed in the natural gas network model in Section 3, is approximated by applying *Wendroff* difference to the partial differential momentum and material-balance equations, and the approximation has the 2nd order accuracy with the truncation error $O(\Delta t^2)$ [20]. Consequently, a smallerΔt is preferred to derive more accurate results, at the costs of higher memory needs and heavier computational burden. In the simulations of this paper, Δt is set as 120 s, i.e., in each of the n_T hours dynamic gas variables will be calculated in every 2 min for a total of 30 times. Within the time period of one hour, minute-scale mass flow rates at gas nodes of P2G assets and gas-fired generators are coupled with the corresponding electric power consumption of P2G and electric power generation of gas-fired generators in that hour. As shown in Fig. 2, the hour-scale electricity variables and the minute-scale gas variables are included in a single scheduling framework. As time goes by, the short-term scheduling time window is moved forward by 1 h.

3. Multi-timescale coordinated scheduling models of IEGS

In the IEGS, the electricity network is composed of gas-fired generators, wind turbines, other non-gas-fired generators, as well as non-P2G and P2G electricity loads. The natural gas network includes P2G and non-P2G gas sources as well as non-generation and generation gas demands. The aims of multi-timescale coordinated scheduling are twofold, i.e. improving economic efficiency and accommodating wind power uncertainties, with the potential flexibility offered by linepack of the natural gas network.

3.1. Optimal short-term scheduling model

- Objective

The objective of short-term coordinated scheduling is to minimize the total operation costs during the entire scheduling period. The operation cost of IEGS includes two components, i.e. the cost of purchasing natural gas from non-P2G gas sources to supply non-generation and generation gas demands, and the operational cost of electricity generators to satisfy non-P2G and P2G electricity demands. The objective function is given as in (1).

$$\min \sum_{T=1}^{n_T} \sum_{n \in S_{eg}} cp_{n,T} P_{n,T} + \sum_{t=1}^{n_t} \sum_{s \in S_{gs}} cg_{s,t} M_{s,t} \Delta t \tag{1}$$

where T and n_T are time index and total number of time periods for hour-scale based electricity variables; t and n_t are time index and total number of time periods for minute-scale based natural gas variables, where $n_t = 30 \cdot n_T$; $cp_{n,T}$ and $P_{n,T}$ are the cost coefficient and active power of electricity generator n at time T; S_{eg} is the set of electricity generators; $cg_{s,t}$ and $M_{s,t}$ are the cost coefficient and mass flow rate of gas source s at time t; S_{gs} is the set of non-P2G gas sources. For wind turbines, $cp_{n,T}$ is set to zero for accommodating renewable energy preferentially; for gas-fired generators, $cp_{n,T}$ is set to zero since its operation cost is considered in terms of gas fuel costs in the natural gas system.

- Operational Constraints

(i) Constraints for Energy Coupling Components

In IEGS, electricity and natural gas networks are coupled via P2Gs and gas-fired generators. These two sets of assets are scheduled to work complementarily for meeting electricity and gas demands while achieving economic operations. Their operational characteristics are modelled as follows.

P2G can convert electricity to natural gas, and the relationship between the consumed mass flow rate and the generated electricity power can be formulated as in (2).

$$M_{n,t}^{ws} = \eta_n P_{n,T}^{ws},\ t = 3600(T-1)/\Delta t + 1,\ \cdots, 3600T/\Delta t;\ T = 1,\ \cdots, n_T;\ n \in S_{\mathrm{p2g}};\ ws \in S_{\mathrm{w}} \tag{2}$$

where S_{p2g} is the set of P2Gs; S_{w} is the set of wind power scenarios including the forecasting and the extreme ones; η_n is energy conversion coefficient of P2G n from electricity to natural gas; $P_{n,T}^{ws}$ and $M_{n,t}^{ws}$ are the consumed electricity power and the generated natural gas mass flow rate of P2G n in wind power scenario ws. The time indices T and t for P2G variables $P_{n,T}^{ws}$ and $M_{n,t}^{ws}$ are different and are coupled via (2).

A gas-fired generator consumes natural gas to generate electricity, as depicted as in (3).

$$M_{i,t}^{ws} = \alpha_i P_{i,T}^{ws},\ T = [(t-1)\Delta t/3600] + 1;\ t = 1,\ \cdots, n_t;\ i \in S_{\mathrm{gg}};\ ws \in S_{\mathrm{w}} \tag{3}$$

where S_{gg} is the set of gas-fired generators; α_i is energy conversion coefficient of gas-fired generator i; $M_{i,t}^{ws}$ and $P_{i,T}^{ws}$ are the consumed mass flow rate and the generated electric power of gas-fired generator i in wind power scenario ws. Constraint (3) describes the coupling relationship between variables $P_{i,T}^{ws}$ and $M_{i,t}^{ws}$ at different timescales.

(ii) Constraints of the Electricity Network

For the hour-scale electricity network formulation, DC power flow based steady-state model (4) is considered.

$$Pf_{l,T}^{ws} - \frac{\Delta\theta_{l,T}^{ws}}{x_l} = 0,\ l \in S_{\mathrm{el}};\ ws \in S_{\mathrm{w}};\ T = 1,\ \cdots, n_T \tag{4}$$

where S_{el} is the set of electricity transmission lines; $Pf_{l,T}^{ws}$ is power flow through line l at time T in wind power scenario ws; $\Delta\theta_{l,T}^{ws}$ is voltage phase angle difference between the two buses connecting line l; x_l is the reactance of line l.

Power flow through electricity transmission line l is constrained by its capacity limit as in (5).

$$-Pf_l^{\max} \leqslant Pf_{l,T}^{ws} \leqslant Pf_l^{\max},\ l \in S_{\mathrm{el}};\ ws \in S_{\mathrm{w}};\ T = 1,\ \cdots, n_T \tag{5}$$

where $Pf_l^{\max}$ is the power flow capacity of line l.

Voltage phase angle at bus b is limited as in (6).

$$\theta_b^{\min} \leqslant \theta_{b,T}^{ws} \leqslant \theta_b^{\max},\ b \in S_{\mathrm{eb}};\ ws \in S_{\mathrm{w}};\ T = 1,\ \cdots, n_T \tag{6}$$

where S_{eb} is the set of electricity buses.

The supply and demand balance of real power at bus b needs to be satisfied as in (7).

$$P_{\mathrm{net},b,T}^{ws} = \sum_{l \in L_b} Pf_{l,T}^{ws},\ b \in S_{\mathrm{eb}};\ ws \in S_{\mathrm{w}};\ T = 1,\ \cdots, n_T \tag{7}$$

where $P_{\mathrm{net},b,T}^{ws}$ is net power injection at bus b at time T in wind power scenario ws; $l \in L_b$ represent the branches that are directly connected with bus b.

(iii) Unit Commitment Constraints

Unit commitment constraints for a non-gas fired generator is represented in (8)–(14). For gas-fired generators, constraints (8)–(14) still apply while all variables will be super-indexed by ws, i.e., as gas-fired generators are used to mitigate wind power uncertainties, their decision variables are dependent on wind power scenario ws.

Power generation of an electricity generator is limited by its upper and lower bounds, presented as in (8).

$$I_{n,T} P_n^{\min} \leqslant P_{n,T} \leqslant I_{n,T} P_n^{\max},\ n \in S_{\mathrm{eg}};\ T = 1,\ \cdots, n_T \tag{8}$$

where $I_{n,T}$ is binary unit commitment variable for electricity generator n.

Introducing binary startup/shutdown variables $B_{n,\tau}^{\mathrm{SU}}$ and $B_{n,\tau}^{\mathrm{SD}}$ for electricity generator, minimum up and down time constraints can be formulated as in (9) and (10):

$$\sum_{\tau=\max\{1, T-TU_n+1\}}^{T} B_{n,\tau}^{\mathrm{SU}} \leqslant I_{n,T}, n \in S_{\mathrm{eg}};\ T = 1,\ \cdots, n_T \tag{9}$$

$$\sum_{\tau=\max\{1, T-TD_n+1\}}^{T} B_{n,\tau}^{\mathrm{SD}} \leqslant 1 - I_{n,T}, n \in S_{\mathrm{eg}};\ T = 1,\ \cdots, n_T \tag{10}$$

where TU_n and TD_n are minimum up and down times of electricity generator n.

Considering startup/shutdown ramp rates and ramp up/down rates, the following constraints are imposed.

$$P_{n,T} - P_{n,T-1} \leqslant R_n^{+} I_{n,T-1} + R_n^{\mathrm{SU}} B_{n,T}^{\mathrm{SU}},\ n \in S_{\mathrm{eg}};\ T = 1,\ \cdots, n_T \tag{11}$$

$$P_{n,T-1} - P_{n,T} \leqslant R_n^{-} I_{n,T} + R_n^{\mathrm{SD}} B_{n,T}^{\mathrm{SD}},\ n \in S_{\mathrm{eg}};\ T = 1,\ \cdots, n_T \tag{12}$$

where R_n^{+} and R_n^{-} are ramp up and ramp down limit of generator n; R_n^{SU} and R_n^{SD} are startup and shutdown ramp rate of generator n.

In addition, binary unit commitment variables as well as startup and shutdown variables follow the logic constraints as in (13) and (14):

$$0 \leqslant B_{n,T}^{\mathrm{SU}} + B_{n,T}^{\mathrm{SD}} \leqslant 1, n \in S_{\mathrm{eg}};\ T = 1,\ \cdots, n_T \tag{13}$$

$$I_{n,T} - I_{n,T-1} = B_{n,T}^{\mathrm{SU}} - B_{n,T}^{\mathrm{SD}},\ n \in S_{\mathrm{eg}};\ T = 1,\ \cdots, n_T \tag{14}$$

(iv) Constraints for Natural Gas Transmission Dynamics

In the natural gas network, gas transmission dynamics should not be neglected due to its large inertia, while mass flow rates and gas pressures need a much longer time to reach a new steady state. To this end, gas dynamical model is necessary to optimize mass flow rates and gas pressures, guaranteeing these variables are within the required range while minimizing the total operation cost.

The basic principles of fluid dynamics, including material-balance equation and momentum equation, govern the gas transmission along pipeline. They are typically described as partial differential equations, relating the mass flow rates and gas pressures with time and position along the pipeline. With Wendroff difference method [23], the two partial differential equations can be reformulated as following [20].

$$\pi_{j,t+1}^{ws} + \pi_{i,t+1}^{ws} - \pi_{j,t}^{ws} - \pi_{i,t}^{ws} + \frac{c^2 \Delta t}{L_{ij} A_{ij}} \cdot (M_{j,t+1}^{ws} - M_{i,t+1}^{ws} + M_{j,t}^{ws} - M_{i,t}^{ws}) = 0,\ ws \in S_{\mathrm{w}};\ t = 1,\ \cdots, n_t \tag{15}$$

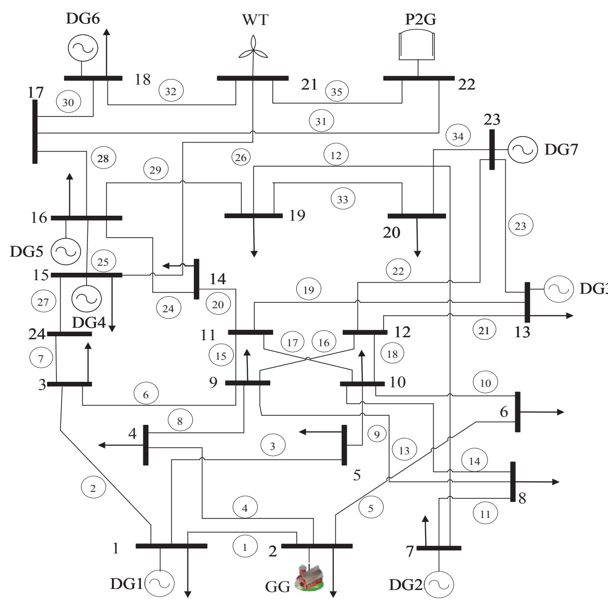

(a) An IEEE 24-bus, 35-branch electricity network.

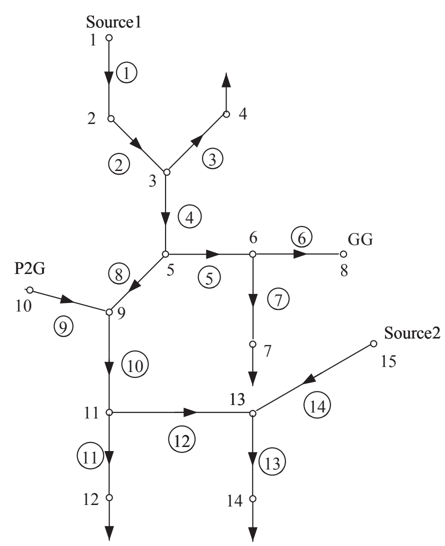

(b) A 15-node, 14-branch natural gas network.

Fig. 3. Topologies of electricity and natural gas networks in IEGS.

$$\frac{c^2}{A_{ij}}(M_{j,t+1}^{ws}+M_{i,t+1}^{ws}-M_{j,t}^{ws}-M_{i,t}^{ws})+\frac{\Delta t}{L_{ij}}\cdot(\pi_{j,t+1}^{ws}-\pi_{i,t+1}^{ws}+\pi_{j,t}^{ws}-\pi_{i,t}^{ws})+\frac{c^2\lambda\Delta t\varpi_{ij}^{ws}}{4d_{ij}A_{ij}}\cdot(M_{j,t+1}^{ws}+M_{i,t+1}^{ws}+M_{j,t}^{ws}+M_{i,t}^{ws})=0, ws\in S_{\mathrm{w}};\ t=1,\ \cdots,n_t \tag{16}$$

where $\varpi_{ij}^{ws}=c^2(M_{i,t}^{ws}/\pi_{i,t}^{ws}+M_{j,t}^{ws}/\pi_{j,t}^{ws})/(2A_{mn})$ is the average gas flow rate; pressure π and density ρ satisfy $\pi=c^2\rho$ and $c^2=RTZ$, in which the parameters of gas constant R, temperature T, and compressibility factor Z are set as $R=500$, $T=273$ K, and $Z=0.9$.

For a joint node in the natural gas network that connects multiple pipelines, Eq. (17) describes the mass flow rate balance, i.e. the total mass inflow should be equal to the total outflow.

$$M_{i,t}^{ws}+M_{i+1,t}^{ws}+M_{i+2,t}^{ws}+...=0, ws\in S_{\mathrm{w}};\quad t=1,\ \cdots,n_t \tag{17}$$

Gas pressure at the joint node should also be consistent.

$$\pi_{i,t}^{ws}=\pi_{i+1,t}^{ws}=\pi_{i+2,t}^{ws}=\cdots, ws\in S_{\mathrm{w}};\ t=1,\ \cdots,n_t \tag{18}$$

Mass flow rates and gas pressures at each node i should be confined to their upper and lower limits.

$$M_i^{\min}\leqslant M_{i,t}^{ws}\leqslant M_i^{\max}, ws\in S_{\mathrm{w}}; t=1,\ \cdots,n_t \tag{19}$$

$$\pi_i^{\min}\leqslant \pi_{i,t}^{ws}\leqslant \pi_i^{\max}, ws\in S_{\mathrm{w}};\ t=1,\ \cdots,n_t \tag{20}$$

Mass flow rates $M_{i,t}$ at non-generation gas demand nodes are fixed as given input $MD_{i,t}$.

$$M_{i,t}=MD_{i,t},\ i\in S_{\mathrm{ngd}}; t=1,\ \cdots,n_t \tag{21}$$

In the natural gas network model, only mass flow rates at non-P2G gas source nodes are independent of wind power scenarios ws, other mass flow rates and pressures rely on ws.

In summary, in short-term scheduling model, power generation of non-gas-fired generators and non-P2G gas sources are identical for different scenarios, while those of gas-fired generators and P2G gas sources are scenario dependent, serving as the mitigator of uncertain wind power scenarios.

3.2. Optimal real-time dispatching model

For the sake of discussion, it is assumed that time-resolution of wind power fluctuations is the same that of gas dynamics Δt. Indeed, if they are different, a multi-timescale integrated dispatching method similar to the one used in above for short-term scheduling can be implemented. In real-time dispatching, the realization of wind power would differ from its hourly forecasting value because of prediction errors. In order to mitigate impacts of such prediction errors on short-term scheduling results of non-P2G gas sources and non-gas-fired generators, operations of P2G assets and gas-fired generators are adaptively adjusted to ensure that gas pressures deviate from their short-term scheduled values as small as possible.

The optimization objective is described as in (22).

$$\min \sum_{i\in S_{\mathrm{gn}}}\sum_{t=1}^{rt}(\pi_{i,t}^{r}-\overline{\pi}_{i,t})^2 \tag{22}$$

where S_{gn} is the set of gas network nodes, rt is the number of time periods for real-time dispatch, $\overline{\pi}_{i,t}$ is the average value of gas pressures for individual wind power scenario obtained from the short-term schedule model. In real-time dispatch, the constraints include (4)–(7), (8)–(14) for gas-fired generators, and (15)–(21).

For each uncertain wind power scenario, with the short-term scheduling results for non-gas-fired generators and non-P2G gas sources, the real-time dispatch is implemented to optimize the operation of P2G assets and gas-fired generators. In the dispatching time horizon of 1 h, if gas pressures at certain gas network nodes are beyond their limits for a certain time, the corresponding wind power scenario is regarded as extreme one. The discovered extreme scenarios are sent back to the short-term schedule problem for re-optimization.

The short-term scheduling and the real-time dispatching are formulated as mixed integer linear programming (MILP) problems and can be solved by Cplex.

4. Simulation results

In this work, an IEGS shown in Fig. 3 is established to illustrate the effectiveness of the proposed multi-timescale coordinated scheduling approach, considering steady-state electricity power flow and gas delivery dynamics. The studied IEGS is composed of an IEEE 24-bus, 35-branch electricity network and a 15-node, 14-branch natural gas network. The electricity network includes one gas-fired generator (GG) at node 2, one wind turbine (WT) at node 21, one P2G asset at node 22, and seven non-gas-fired generators denoted by DG1-DG7. The electricity network is coupled with the gas network via GG and P2G, serving as gas load and source at gas nodes 8 and 10, respectively. The natural gas network includes 2 non-P2G gas sources located at gas nodes 1 and 15, as well as 4 non-generation gas loads at gas nodes 4, 7, 12, and 14. For DG1-DG7 and GG, the maximum ramp up/down rate and startup/shutdown ramp rates are half of their corresponding capacity limits; and their minimum up/down times are set as 2 h and 1 h, respectively. The energy conversion coefficients of P2G and GG are set as $\eta = 0.115$ and $\alpha = 0.075$.

The following three cases are designed to show advantage of the proposed electricity and gas coupled short-term scheduling approach under various energy prices, gas source failures, and gas demand surges, which coordinates gas-fired generators, non-gas fired generators, P2Gs, non-P2G gas sources, and gas linepack to achieve economic operation while satisfying the electricity and gas demands:

- Case 1: This is the base case to study the proposed coordinated optimal scheduling approach.
- Case 2: This case, as compared to Case 1, illustrates the impacts of higher non-gas fired generation costs and non-P2G gas source failures on the optimal short-term scheduling results and discovers the role of linepack.
- Case 3: This case, as compared to Case 1, studies the impacts of lower non-gas fired generation costs and higher non-generation gas loads on the optimal short-term scheduling results.

In Cases 1–3, solutions of variables for P2G and GG are values corresponding to the forecasted wind power scenario. Moreover, the third hour in Case 1 is taken as an example to further discuss the necessity of coordinating short-term scheduling and real-time dispatching to ensure operational security and economics of the IEGS.

4.1. Case 1

A short-term scheduling horizon of 4 h is considered since 4-hour timespan is usually used in short-term scheduling of electric power systems. During the period of 4 h, price of natural gas from gas source is fixed as 4 Yuan/kg, while cost of DG1-DG7 is set as 1.8 Yuan/kWh during hours 1–2 and reduced to 0.6 Yuan/kWh during hours 3–4. First, the short-term scheduling is implemented only considering the forecasting of wind power. Then, with the short-term scheduling results, real-time dispatching is conducted and extreme wind power scenarios are identified and fed back to short-term scheduling until no extreme scenarios are discovered. The derived results of electricity and natural gas variables considering the forecasting and extreme scenarios of wind power are given in Figs. 4–7.

Fig. 4 shows that aiming to achieve the economic optimization, during hours 1–2 the electricity power consumption of P2G is smaller since the cost of consuming electricity to produce gas is less cost-efficient than directly utilizing natural gas from gas sources; and

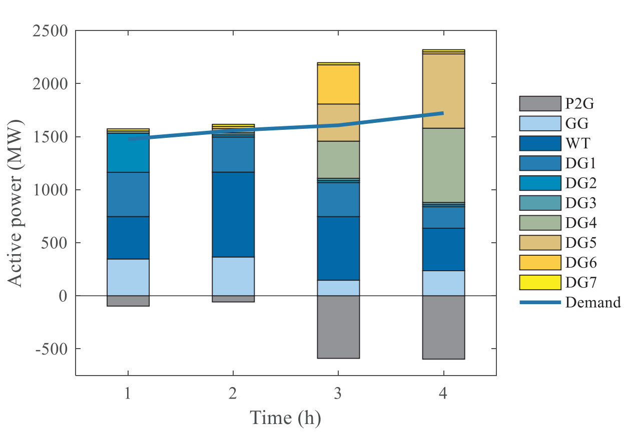

Fig. 4. Short-term scheduling results of electricity power generation in Case 1.

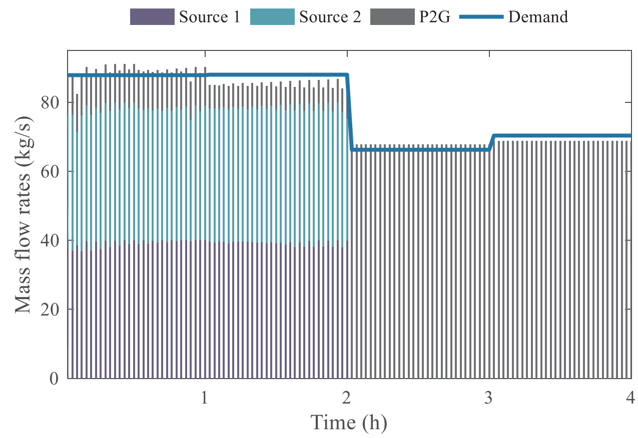

Fig. 5. Short-term scheduling results of mass flow rates in Case 1.

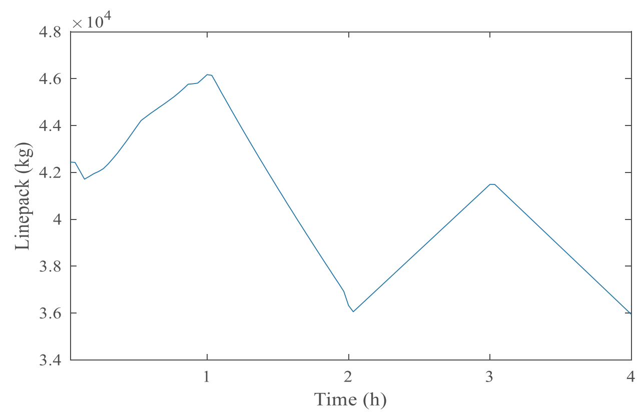

Fig. 6. Short-term scheduling results of natural gas linepack in Case 1.

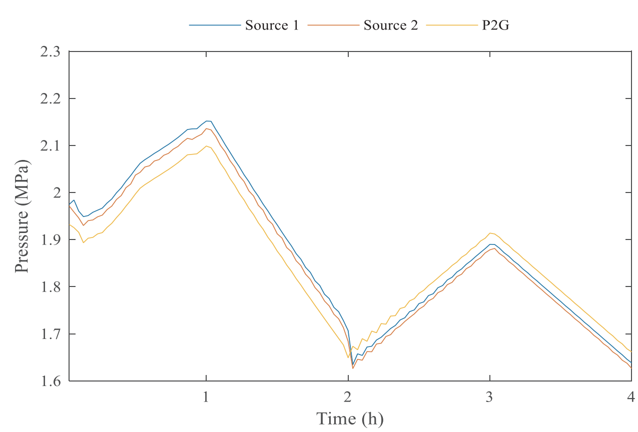

Fig. 7. Short-term scheduling results of pressures at P2G and gas sources nodes in Case 1.

simultaneously, electricity generation from GG is higher. On the contrary, during hours 3–4 the electricity consumption of P2G increases sharply to satisfy all natural gas demands by using cheaper electricity power; while power output from GG declines significantly.

Natural gas mass flow rates from the two gas sources and P2G are depicted in Fig. 5. It is discovered that, during hours 1–2 natural gas mass flow rate from P2G is very low; and during hours 3–4, due to the cheaper gas generation from P2G, the mass flow rates from both Sources 1 and 2 almost drop to zero to achieve the minimal total operational cost. Moreover, for all hours, mismatch between supply and demand gas mass flow rates exists, resulting in linepack variation, i.e. the volume of natural gas stored in pipeline, as shown in Fig. 6.

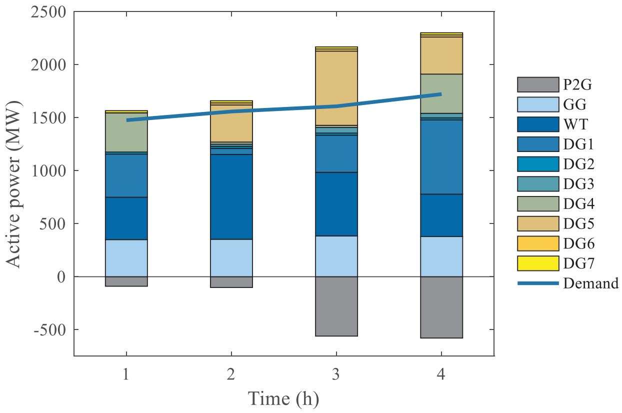

Fig. 8. Short-term scheduling results of electricity power in Case 2.

Comparing Figs. 5 and 6 we can see that the linepack increases when the net gas mass inflow is positive and decreases when it is negative. Natural gas pressures at the nodes of gas sources and P2G are depicted in Fig. 7, constrained by the limit of $1.63\text{MPa} \leqslant \pi_i \leqslant 2.25\text{MPa}$. Aiming at the economic operation, as shown in Fig. 7, the pressures at gas sources are close to their lower limits at the end of scheduling period. Fluctuations of pressures are also guaranteed to be within the operational range by imposing corresponding constraints in the MILP model. In addition, Figs. 6 and 7 indicate that pressures at gas sources and P2G show the similar variation trend as the linepack.

4.2. Case 2

In this case, for all 4 h, electricity generation cost of DG1-DG7 is 1.8 Yuan/kWh and price of natural gas from the two gas sources are kept as 4 Yuan/kg. In addition, during hours 1–2, the two gas sources are in normal operation; while during hours 3–4, both gas sources face with certain partial failures, reducing their mass flow rate upper limits to 8 kg/s.

The short-term scheduling results of electricity power generation are shown in Fig. 8. The electricity generation from GG is large during the whole scheduling period due to higher electricity generation costs of DG1-DG7. The scheduling results of natural gas mass flow rates are depicted in Fig. 9. As shown in Figs. 8 and 9, during hours 1–2, gas generation from P2G is low because purchasing natural gas from gas sources is cheaper than generating natural gas by consuming electricity. However, during hours 3–4, because the gas supply shortage from Sources 1 and 2, gas generation from P2G has to increase sharply to satisfy gas demand, which almost reaches its maximum mass flow rate

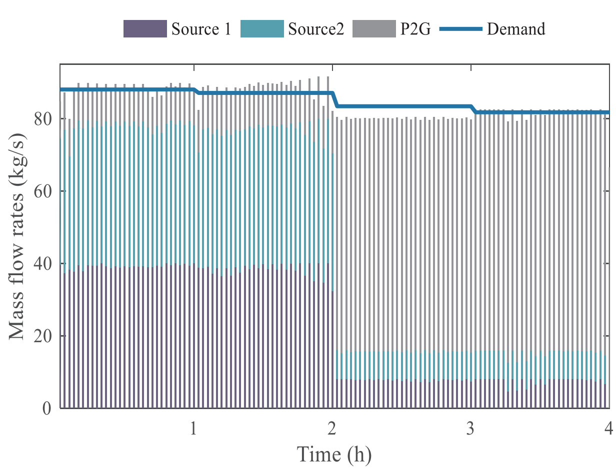

Fig. 9. Short-term scheduling results of mass flow rates in Case 2.

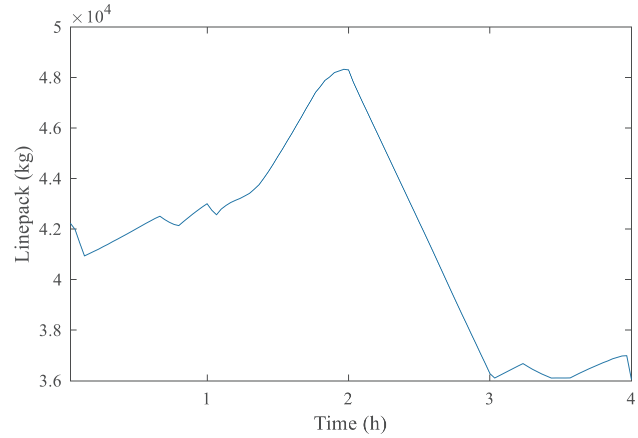

Fig. 10. Short-term scheduling results of natural gas linepack in Case 2.

although not cost-effective. The linepack in gas pipeline is shown in Fig. 10, which illustrates the flexibility offered by linepack of the gas network to meet gas needs of the IEGS. As shown in Fig. 10, in order to achieve the minimum operation cost during the whole scheduling period, the linepack at hours 1–2 keeps increasing and at the end of hour 2, the linepack almost reaches its highest level, aiming to store cheaper gas into the pipeline in advance and provide gas supply during hours 3–4 when gas sources are not fully available. In addition, gas pressures at the nodes of P2G and the two gas sources are depicted in Fig. 11, which represent similar variation trend as linepack while constrained by the operation limit. Comparing Figs. 4 and 8, it can be observed that although in Cases 1 and 2 prices and energy demands at hour 2 are identical, P2G electricity consumption at hour 2 in Case 2 is about 101.67 MW, much higher than 58.21 MW in Case 1. Accordingly, as shown in Fig. 9, during hour 2 the total gas supply is higher than demand, different from that in Fig. 5, which means that the gas network works in the charging mode during hour 2 to store gas in advance and be prepared for the coming gas source failure.

4.3. Case 3

In this case, for all 4 h, electricity generation cost of DG1-DG7 is 0.6 Yuan/kWh and price of natural gas from the two gas sources are kept as 4 Yuan/kg, indicating that the electricity energy is cheaper than natural gas energy. In addition, during hours 3–4, gas demands at nodes 4, 7, 12, and 14 are increased to almost twice as much as hours 1–2.

The scheduling results of electricity generation and gas mass flow rates are given in Figs. 12 and 13. In order to achieve the optimal economic objective under the current energy prices, during the entire

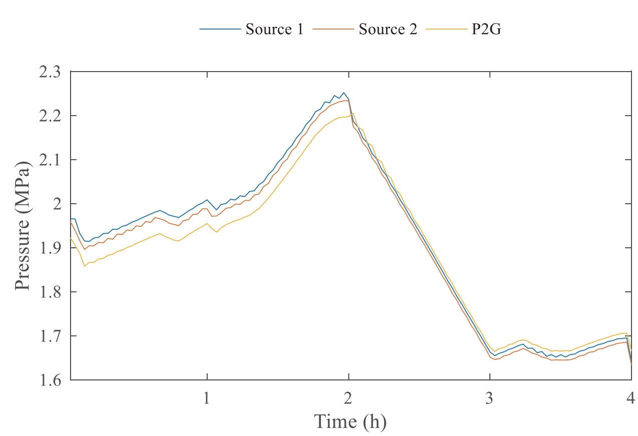

Fig. 11. Short-term scheduling results of pressures at P2G and gas sources nodes in Case 2.

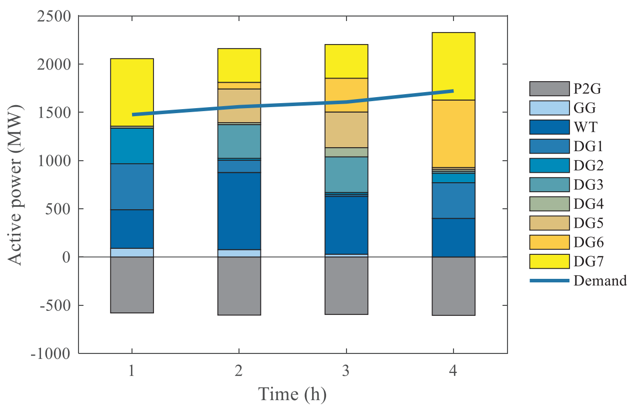

Fig. 12. Short-term scheduling results of electricity power in Case 3.

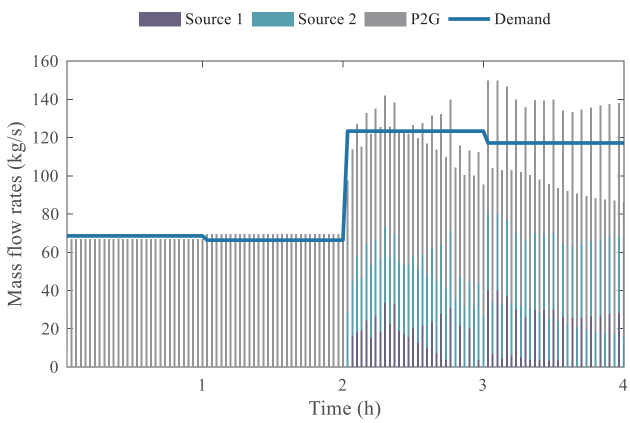

Fig. 13. Short-term scheduling results of mass flow rates in Case 3.

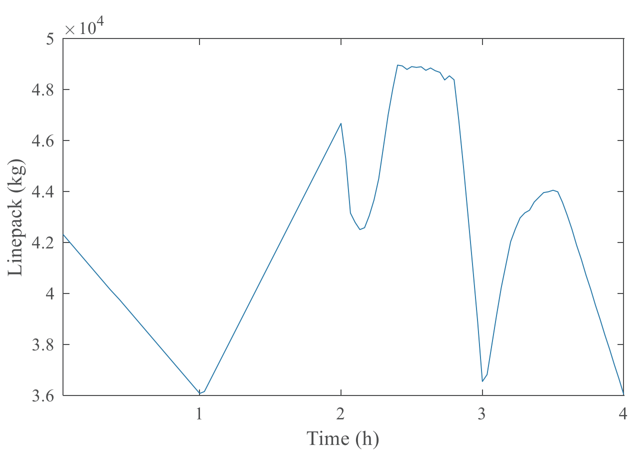

Fig. 14. Short-term scheduling results of natural gas linepack in Case 3.

scheduling period, the P2G asset keeps a higher level of electricity consumption, especially different from that during hours 1–2 in Cases 1 and 2. On the contrary, due to its higher operation cost, the total electricity generation from GG is lower than those in Cases 1 and 2, supplying a negligible proportion of total electricity demand during hours 1–4. Accordingly, during hours 1–2, mass flow rates from the two gas Sources 1 and 2 are zero, and all gas demands are satisfied by the P2G generation. During hours 3–4, the gas demand surges and cannot be fully supplied by the P2G, constrained by its maximum mass flow rate limit of 70 kg/s in short-term scheduling. As a result, contrasting with Case 1, two gas sources start to fill the gap between gas demand and maximum gas supply from P2G, although non-P2G gas source is not cost-effective. The linepack in gas pipeline is shown in Fig. 14, which

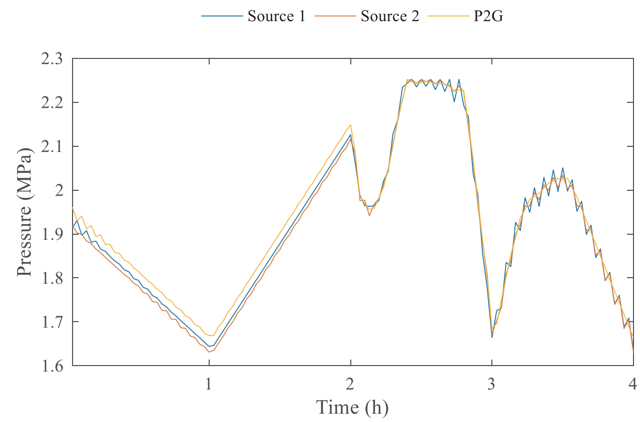

Fig. 15. Short-term scheduling results of pressures at P2G and gas sources nodes in Case 3.

reaches a relatively high level, almost 47000 kg, at the end of hour 2. The pressures at P2G and gas source nodes are shown in Fig. 15, both of which present similar variation trend as linepack.

4.4. Discussions on the necessary of coordinating short-term scheduling and real-time dispatching

We further take hour 3 in Case 1 as an example to describe the effectiveness of the coordinated short-term scheduling and real-time dispatching in mitigating wind power uncertainties. Wind power uncertainties are assumed to follow normal distribution $N(600, 100)$, and 100 scenarios are generated by Latin Hypercube Sampling (LHS) method [24]. Other statistical distribution, such as Weibull, Rician, and Rayleigh distribution, can be considered in a similar fashion.

First, the short-term scheduling without considering extreme wind power scenarios is implemented. The scheduled pressures at P2G and gas source nodes are depicted in Fig. 16. With the short-term scheduling results, 5 extreme scenarios from the original 100 scenarios are identified by solving the real-time dispatching problem, indicated in Fig. 17. Specifically, for the worst extreme scenario s1, the real-time dispatched pressures at gas sources and P2G nodes are shown in Fig. 18, with pressure violation lasting for over 20 min. In this study, we apply the strategy of adding only the scenario with the least violation back to the short-term scheduling problem to avoid over-conservativeness. Among the 5 extreme scenarios, the real-dispatched node pressure constraint violation in scenario s2 is the least. After considering s2 in short-term scheduling, the corresponding new operation solution will derive no further extreme scenarios in real-time dispatching. Specifically, when applying this new operation solution to the worst extreme scenario s1

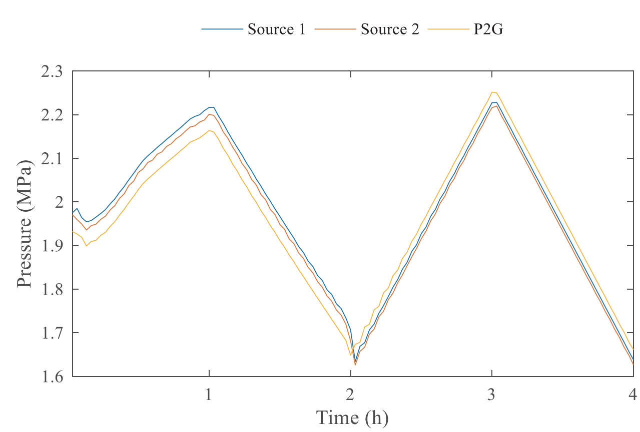

Fig. 16. Short-term scheduling results of pressures at P2G and gas sources nodes in Case 1 without considering extreme scenarios.

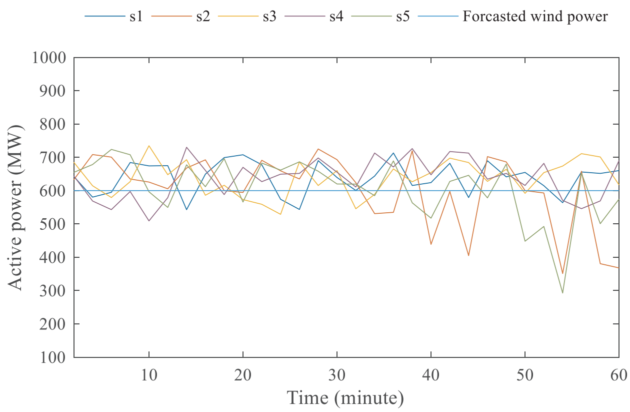

Fig. 17. Forecasted wind power and the discovered extreme scenarios during hour 3 in Case 1.

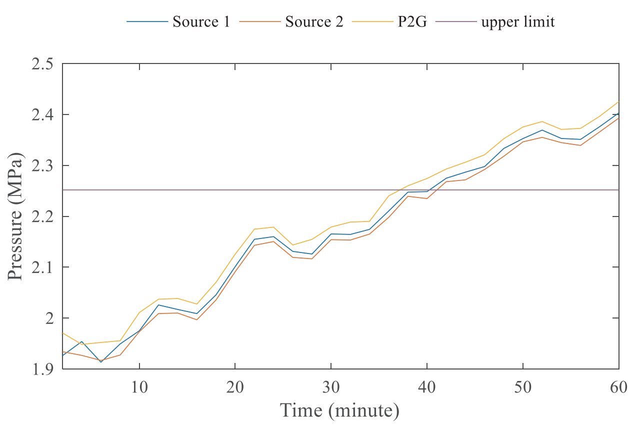

Fig. 18. Real-time dispatched pressures at P2G and gas sources nodes for s1 without considering extreme scenarios in short-term scheduling.

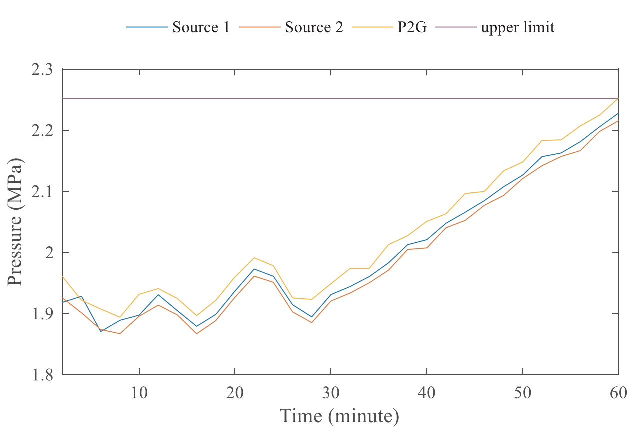

Fig. 19. Real-time dispatched pressures at P2G and gas sources nodes for s1 after considering extreme scenarios in short-term scheduling.

identified in the previous iteration, pressures at gas sources and P2G nodes from the real-time dispatching are drawn in Fig. 19. No pressure violation is observed, although the pressure at P2G node almost reaches

Appendix A

(See Tables 1–3).

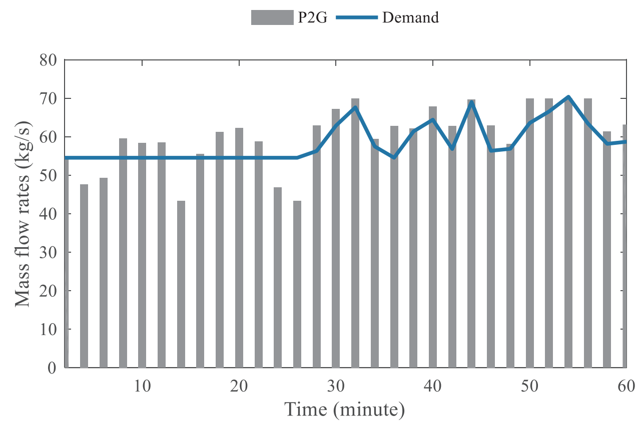

Fig. 20. Real-time scheduling results of mass flow rates for s1 after considering extreme scenarios in short-term scheduling.

its upper limit. The real-time dispatching results of mass flow rate are shown in Fig. 20. As indicated in Fig. 20, the unbalance of mass flow rate supply and demand exists all the time and consequently the pressures fluctuate. During 26th-60th min of hour 3, the gas demand variation is caused by the gas consumption of gas-fired generation. Figs. 16 and 7 clearly show that considering extreme scenarios in the short-term scheduling, although sacrificing certain economics, can lead to a wider secure margin of nodal pressures, which could provide linepack of more flexibility to smooth fluctuations of uncertain wind power in real-time dispatching.

5. Conclusion

A multi-timescale coordinated scheduling framework for IEGS is proposed in this paper, in which electricity and natural gas supplies can be simultaneously scheduled economically by considering the coupling bought by P2G assets and gas-fired generators, while effectively mitigating wind power uncertainties by leveraging flexibility offered by P2G assets, gas-fired generators, and gas linepack. In the multi-timescale integrated scheduling, the short-term scheduling is coordinated with real-time dispatching to achieve economic operation and smooth wind power fluctuation, with extreme wind power scenarios identified by real-time dispatching and sent back to short-term scheduling. In short-term scheduling, hourly-scale steady-state power flow and minute-scale dynamic gas transmission are integrated in a unified optimization model to capture the coupling relations of energy conversions at each time slot during scheduling horizon, which makes it easy to quantitatively analyze the effect of gas linepack on economic scheduling and uncertain wind power mitigation. In the coordination scheduling approach, the co-optimized strategy of electricity generations and gas source supplies can be achieved under various situations, such as different generation and gas costs as well as the gas source inadequacy due to gas source outages and gas demand surges. With the proposed multi-timescale coordinated scheduling framework of IEGS, the linepack of natural gas network can be scheduled to act as an energy storage to help pursue economic operation objective and smooth wind power fluctuations. In summary, the proposed approach could provide valuable insights into the economic and reliable operation of IEGS with uncertain renewable energy.

Table 1
Parameters of natural gas network.

Parameter	Value
pipeline length L	1000 m
pipeline diameter d	0.5 m

Table 2
Gas load in natural gas network in Cases 1 and 2.

Time (h)	Gas load (kg/s)			
	Node 4	Node 7	Node 12	Node 14
Hour 1	11.9340	13.1580	17.9010	18.8190
Hour 2	11.7000	12.9000	17.5500	18.4500
Hour 3	10.5300	11.6100	15.7950	16.6050
Hour 4	10.2960	11.3520	15.4440	16.2360

Table 3
Gas load in natural gas network in Case 3.

Time (h)	Load demand (kg/s)			
	Node 4	Node 7	Node 12	Node 14
Hour 1	11.9340	13.1580	17.9010	18.8190
Hour 2	11.7000	12.9000	17.5500	18.4500
Hour 3	23.4000	25.8000	35.1000	36.9000
Hour 4	22.6200	24.9400	33.9300	35.6700

References

[1] Xu X, Jia HJ, Chiang HD, Yu DC, Wang D. Dynamic modeling and interaction of hybrid natural gas and electricity supply system in microgrid. IEEE Trans Power Syst May 2015;30(3):1212–21.

[2] Saldarriaga CA, Hincapié RA, Salazar H. A holistic approach for planning natural gas and electricity distribution networks. IEEE Trans Power Syst Nov. 2013;28(4):4052–63.

[3] Clegg S, Mancarella P. Integrated modeling and assessment of the operational impact of power-to-gas (P2G) on electrical and gas transmission networks. IEEE Trans Sustain Energy Oct. 2015;6(4):1234–44.

[4] Zhang X, Che L, Shahidehpour M, Alabdulwahab AS, Abusorrah A. Reliability-based optimal planning of electricity and natural gas interconnections for multiple energy hubs. IEEE Trans Smart Grid Jul. 2017;8(4):1658–67.

[5] Dokic SB, Rajakovic NL. Security modelling of integrated gas and electrical power systems by analyzing critical situations and potentials for performance optimization. Energy May 2018. https://doi.org/10.1016/j.energy.2018.04.165.

[6] Ameli H, Qadrdan M, Strbac G. Value of gas network infrastructure flexibility in supporting cost effective operation of power systems. Appl Energy Sep. 2017;202:571–80.

[7] He Y, Shahidehpour M, Li Z, Guo C, Zhu B. Robust constrained operation of integrated electricity-natural gas system considering distributed natural gas storage. IEEE Trans Sustain Energy Jul. 2017;9(3):1061–71.

[8] A. Martínez-Mares and C. R. Fuerte-Esquivel, “Integrated energy flow analysis in natural gas and electricity coupled systems,” In 2011 North American Power Symposium, Aug. 2011, pp. 1-7.

[9] Martinez-Mares A, Fuerte-Esquivel CR. A unified gas and power flow analysis in natural gas and electricity coupled networks. IEEE Trans. Power Syst Nov. 2012;27(4):2156–66.

[10] Chaudry M, Jenkins N, Qadrdan M, Wu J. Combined gas and electricity network expansion planning. Appl Energy Jan. 2014;113:1171–87.

[11] Shao C, Shahidehpour M, Wang X, Wang X, Wang B. Integrated planning of electricity and natural gas transportation systems for enhancing the power grid resilience. IEEE Trans Power Syst Nov. 2017;32(6):4418–29.

[12] Qiao Z, Guo Q, Sun H, Pan Z, Liu Y, Xiong W. An interval gas flow analysis in natural gas and electricity coupled networks considering the uncertainty of wind power. Appl Energy Sep. 2017;201:343–53.

[13] Devlin J, Li K, Higgins P, Foley A. A multi vector energy analysis for interconnected power and gas systems. Appl Energy Apr. 2017;192:315–28.

[14] Li G, Zhang R, Jiang T, Chen H, Bai L, Li X. Security-constrained bi-level economic dispatch model for integrated natural gas and electricity systems considering wind power and power-to-gas process. Appl Energy May 2017;194:696–704.

[15] X. Zhang, L. Che and M. Shahidehpour, “Impact of natural gas system on short-term scheduling with volatile renewable energy,” In 2015 IEEE Power & Energy Society General Meeting, Jul. 2015, pp. 1-5.

[16] Correa-Posada CM, Sanchez-Martin P, Lumbreras S. Security-constrained model for integrated power and natural-gas system. J. Mod Power Syst Clean Energy Apr. 2017;5(3):326–36.

[17] Chiang NY, Zavala VM. Large-scale optimal control of interconnected natural gas and electrical transmission systems. Appl Energy Apr. 2016;168:226–35.

[18] Pambour KA, Erdener BC, Bolado-Lavin R, Dijkema GP. SAInt–A novel quasi-dynamic model for assessing security of supply in coupled gas and electricity transmission networks. Appl Energy Oct. 2017;203:829–57.

[19] Zhou Y, Gu C, Wu H, Song Y. An equivalent model of gas networks for dynamic analysis of gas-electricity systems. IEEE Trans Power Syst Nov. 2017;32(6):4255–64.

[20] Fang J, Zeng Q, Ai X, Chen Z, Wen J. Dynamic optimal energy flow in the integrated natural gas and electrical power systems. IEEE Trans Sustain Energy Jun. 2017;9(1):188–98.

[21] Chen D, Bao Z, Wu L. Integrated coordination scheduling framework of electricity-natural gas systems considering electricity transmission $N-1$ contingencies and gas dynamics. J Mod Power Syst Clean Energy 2019;7(6):1422–33.

[22] Yang J, Zhang N, Kang C, Xia Q. Effect of natural gas flow dynamics in robust generation scheduling under wind uncertainty. IEEE Trans Power Syst Mar. 2017;33(2):2087–97.

[23] Gourlay AR, Morris JLl. Finite-difference methods for nonlinear hyperbolic systems. Math Comput 1968;22(101):28. https://doi.org/10.2307/2004760.

[24] G. D. Wyss and K. H. Jorgensen, “A user's guide to LHS: Sandia's Latin Hypercube Sampling Software,” Sandia National Laboratories, Albuquerque, NM, Tech. Rep. SAND98-0210, 1998.